University of
Strathclyde
Glasgow

Strathprints Institutional Repository

http://strathprints.strath.ac.uk/

Effect of sample thickness on the extracted near-infrared bulk optical properties of *Bacillus subtilis* in liquid culture

Elitsa Dzhongova[1], Colin R. Harwood[2], Suresh N. Thennadil[3*]

[1]School of Chemical Engineering and Advanced Materials, Newcastle University, Newcastle upon Tyne, United Kingdom

[2]Institute for Cell and Molecular Biosciences, Newcastle University, Newcastle upon Tyne, United Kingdom

[3]Department of Chemical and Process Engineering, University of Strathclyde, Glasgow, United Kingdom

* Correspondence to Suresh N. Thennadil. Email: suresh.thennadil@strath.ac.uk

ABSTRACT

In order to determine the bulk optical properties of a *Bacillus subtilis* culture during growth phase we investigated the effect of sample thickness on measurements taken with different measurement configurations, namely total diffuse reflectance and total diffuse transmittance. The bulk optical properties were extracted by inverting the measurements using the radiative transfer theory. While the relationship between reflectance and biomass changes with sample thickness and the intensity (absorbance) levels vary significantly for both reflectance and transmittance measurements, the extracted optical properties show consistent behavior both in terms of the relationship with biomass and magnitude. This observation indicates the potential of bulk optical properties for building models that could be more easily transferable compared to those built using raw measurements.

Keywords: Multiple light scattering, optical properties, radiative transfer theory, fermentation, *Bacillus subtilis*.

INTRODUCTION

In a previous study[1], we demonstrated that the Radiative Transfer Theory (RTT) could be used to extract information on the absorption and scattering properties of actively growing bacteria. When the optical properties of the cells were extracted in the near infrared (1350-1550nm) with a path length of 4mm, problems of convergence arose due to a high noise and/or low signal ratio in parts of the spectrum. As a result reliable estimates of the optical parameters were difficult to obtain. One approach to improve the estimates is to identify the optimal path length (sample thickness), which would provide accurate estimates of the optical parameters. Further, since the ultimate goal of extracting the optical properties is to

build robust calibration models for estimating the concentration of various constituents in the sample, it is important to know how the path length of the sample affects the estimation of the bulk optical properties and thus the performance of the corresponding calibration models. In theory, the extracted bulk optical properties should be the same, to within experimental error, irrespective of the sample thickness provided the extraction routine is stable. In this paper we investigated the effect of sample thickness both on extracted bulk optical properties as well as the raw measurements taken with different configurations, namely total diffuse reflectance (R_d) and total diffuse transmittance (T_d).

MATERIALS AND METHODS

Three growth cycle experiments were carried out using the Gram-positive bacterium *Bacillus subtilis* strain 168, obtained from the Institut Pasteur, Paris. In each experiment, the strain was cultivated in 100ml Spizizen's minimal medium containing trace element solution[2] in a 250 ml Erlenmeyer flask. All the bacterial growth cycle experiments were carried out with the medium at pH of 7.0 ± 0.5, the temperature controlled at $37^0C \pm 0.5$, and in an orbital incubator with an agitation rate of 220rpm. For all the three cultures, data was collected during the growth phase and a total of five samples were taken at approximately 2-hour intervals during the growth phase.

For each sample R_d, T_d and T_c measurements were made using cuvettes with different path lengths (2, 4 and 10mm). These measurements were made using a UV-Vis-NIR spectrophotometer (Cary 5000) equipped with an integrating sphere. The measurements were made over the wavelength range of 950nm - 1850nm with an average integration time of 0.4s, an average signal bandwidth of about 15nm at wavelength intervals of 4nm. The biomass of all samples was measured gravimetrically. The protocol

used for both the spectroscopic measurements and the gravimetric measurements were the same as that used in previous work[1, 2]. Bulk optical properties of the samples were extracted from the measurements using the inverse adding-doubling method to invert the radiative transfer equation. Details of this procedure can be found elsewhere.[1,3-5]

RESULTS AND DISCUSSION

Total diffuse reflectance (R_d) measurements

Figure 1 displays raw diffuse reflectance spectra (in absorbance units) for different sample thicknesses over the course of the cultivations. Measurements with 4mm sample thickness had the highest diffuse reflectance and 10mm the lowest, while the measurements with 2mm was intermediate between the other two path lengths. The fact that changes in reflectance with respect to path length are not ordered in relation to the sample thickness is surprising. The diffuse reflectance spectra, taken with the 2mm path length cuvette, contain three pronounced valleys (at 1070nm, 1280nm, and 1700nm), whereas the third valley (at 1700nm) is flattened out in the case of 4mm and 10mm path length cuvettes. This difference is most likely due to the fact that when the sample thickness is higher, the photons that have penetrated the furthest into the sample have a lower probability of being reflected back, especially in the high absorption region (>1400nm). As a result, the dominant part of the reflected intensity recorded by the detector is due to the portion of incident photons reflected by the front surface of the glass due to Fresnel reflection. The intensity of light that has undergone Fresnel reflection varies weakly with wavelength and thus a flat spectrum is obtained in this spectral region. For the sample thickness of 2mm, the photons that would otherwise have been absorbed at greater depths undergo Fresnel

reflection at the back end of the cuvette and therefore have a greater probability of making it back to the detector.

The largest variation in reflectance spectra over the course of the cultivation occurs for the sample thickness of 10mm at wavelengths in the region 950 – 1150nm. The spread in the data seen for the 10mm samples occur during the growth phase, indicating that during this phase the greatest sensitivity to changes can be observed using R_d measurements. Above 1400nm, only the measurements with a sample thickness of 2mm show features of potential interest, indicating that this thickness is the most suitable for extracting information from reflectance measurements in the first overtone region.

In order to examine the spectral variations over the course of a cultivation in more detail, values for diffuse reflectance (-logR_d) were plotted against biomass at a single wavelength. Two wavelengths were chosen: 1050nm (Figure 2) and 1602nm (Figure 3), respectively, to examine trends in the measurements for the scattering dominated region and absorption dominated region.

Measurements with the 2mm thickness sample (Figure 2a) show that the reflectance increases, corresponding to a decrease in absorbance over the course of the growth phase. The same observation has been made by Ge *et al.*[6], while monitoring cell density from a fed-batch fermentation of *Saccharomyces cerevisiae*. A decrease in –logR_d versus cell mass concentration was shown by the same authors at 810nm. However, it should be noted that the experimental setup and the microorganism used in the Ge study are different from that used in the current work. In their study, the diffuse reflectance was collected with a fiber optic bundle on the outside of a glass vessel fermenter, whereas in this work the spectra

were collected with an integrating sphere setup. Although two different techniques were used, the same trend for diffuse reflectance was observed in the scattering dominated region.

In the case of the measurements obtained with 4mm (Figure 2b) and 10mm (figure 2c) path length cuvettes collected during the growth phase, the $-\log R_d$ values increased with increasing biomass which was the opposite of the trend exhibited by data from 2mm sample thickness. Thus for the growth phase, it was found that sample thickness not only affects the levels of reflected intensity but also affects the nature of relationship of the reflected intensity with respect to biomass concentration.

Values ($-\log R_d$) from the absorption dominated region (1602nm) are shown as a function of biomass in Figures 3a-c. For the measurements with 2mm path length cuvettes (Figure 3a) the $-\log R_d$ value decreases with the increase in biomass, although the relationship is very weak. For the other two sample thicknesses there are no discernible trends in the absorbance values with respect to biomass. This is because the major contribution to the spectra due to changes in biomass comes from changes in the amount of scattering and thus the scattering dominated region will be more sensitive to these changes than the absorbance dominated region.

Total diffuse transmittance (T_d) measurements

Figure 4 displays raw diffuse transmittance spectra (in absorbance units), for 2mm, 4mm, and 10mm sample thicknesses. The absorbance increases with increasing sample thickness as would be expected. Only the measurements with the 2mm path length cuvette have a good signal throughout the wavelength range considered, followed by measurements with

4mm path length cuvette in which the water absorption peak around 1450nm is very noisy. For 10mm thick samples, the region beyond 1350nm is very noisy, indicating that it would not be possible to obtain useful information beyond this wavelength. However, for this thickness, the transmittance signal ($-\log T_d$) in the region 950nm-1350nm was seen to have a much higher variation over the course of the growth phase, indicating that this thickness will have the greatest sensitivity with respect to changes in biomass concentration.

In order to study these variations in greater detail, values for diffuse transmittance were plotted against biomass at wavelengths 1050nm (Figure 5) and 1602nm (Figure 6). At 1050nm wavelength, values ($-\log T_d$) obtained with 2mm thick sample (Figure 5a) during the growth phase do not indicate a clear trend with respect to the increase in biomass while, for the thicker samples, absorbance increases approximately linearly with biomass with a slight nonlinearity visible for the 4mm thickness at the lower end of the biomass concentration. Data from the absorption dominated region (1602nm), shows dependence of $-\log T_d$ with biomass (Figure 6). There is no discernible relationship with biomass for any of the sample thickness. This is due to the fact that the absorbance of water is the major contributor to variations in absorption whereas biomass is the major contributor to the variations in the scattering effect and therefore the scattering dominated region is much more sensitive to biomass than the absorption dominated region.

Bulk scattering coefficient

Figure 7 shows the bulk scattering coefficients (μ_s) obtained during the growth phase of a single cultivation run for sample of different thicknesses. It can be seen that the relative

change in μ_s over the duration of the growth phase is large. In the region of the water peak (1450nm) where calculations were highly influenced by the water absorption, reliable estimates could not be obtained. Also, in the region 1550-1850nm, the extracted bulk scattering coefficients exhibit a high degree of uncertainty as indicated by the high noise in the scattering spectra in this region, and by the fact that μ_s extracted at different times during the growth phase appear to have inconsistent trends in this region. This high degree of uncertainty in the extracted bulk scattering coefficients is probably due to the fact that in the absorption dominated region spectra are much less sensitive to changes in scattering coefficients than to changes in the absorption properties. In the region between 1550nm and 1850nm, only scattering spectra for 2mm and 4mm sample thicknesses are presented, since the high level of noise in the raw measurements for the 10mm thick sample led to convergence problems when attempting to extract the optical properties in this region.

By analogy with the raw measurements, values for μ_s are displayed against biomass for wavelengths of 1050nm (Figure 8) and 1602nm (figure 9) in order to examine in more detail the trends in the scattering spectra. It can be seen that μ_s for 2mm, 4mm, and 10mm show clear linear relationship with respect to the growth phase (Figure 8).

At 1602nm, the 2mm thick samples do not show any significant relationship between μ_s and biomass while a non-linear relationship is evident in the 4mm thick samples. The sensitivity to biomass in the 4mm thick samples, unlike the 2mm samples, may be due to , the photons can travelling deeper into the suspension and encountering more scattering events before exiting from the sample. This raises the contribution of scattering to an extent that the inverse adding-doubling routine is able to converge to a stable value of μ_s. Two

outliers are observed in this region. These are more likely to be due to convergence problem in the inversion rather than to any physical characteristics in the system.

The significance of the results in this section lies in the observation that μ_s values extracted using different sample thickness have similar values and their relationship with biomass is of the same form, irrespective of the sample thickness. This is in contrast to what we observed with the R_d and T_d measurements. In both these cases, there are significant differences in the absorbance levels with different cuvette path lengths (Figures 1 and 4). In addition, in the case of R_d measurements, the functional form of the relationship may vary with different sample thicknesses (Figure 2). This observation has potential implications in terms of calibration transfer. For models built using the raw measurements, different calibration models have to be built even when the sample thickness or measurement configuration change slightly, since the level of absorption and the functional form of the relationship between the measurement and the analyte of interest could change significantly. When optical properties are used, as long as the optical properties are obtained accurately, calibration transfer should be much easier to accomplish, regardless of the sample thickness on which the models are built. In principle, calibration transfer should also be easy to accomplish even when a different set of measurement configurations are used to extract the bulk optical property. The latter is a fundamental property of the sample itself and therefore should not vary according to the type of measurement used to extract it.

Bulk absorption coefficient

9

Figure 10 shows the bulk absorption coefficients (μ_a) during the growth phase of a single cultivation run for the different sample thicknesses. The absorption band of water dominates the spectra since it is the major absorbing species in the sample, and consequently changes in absorption during the growth phase are very small. The absorption coefficients extracted using different sample thicknesses are almost identical in the full region studied (950nm-1850nm). For the 4mm and 10mm thick samples, μ_a could not be extracted in the region of the water peak due to the high level of noise in the raw measurements.

Values for μ_a at 1050nm and 1602nm versus biomass are shown in Figures 11 and 12 respectively. A linear relationship between μ_a and biomass are evident for the 4mm and 10mm thick samples at 1050nm whereas the 2mm samples show a very weak trend, mainly due to the lack of sensitivity resulting from the short path length travelled by the photons being insufficient for them to encounter a high number of cells. Such an increase in the bulk absorption coefficient has also been reported by Beauvoit et al,[7] while estimating optical properties of commercial Baker's yeast. The magnitude of increase in μ_a with increase in biomass is smaller by almost an order of magnitude compared to the changes in μ_s at the same wavelength. In figure 12, the absorption coefficient at 1602nm is plotted against biomass. The values for 10mm thick sample were not extracted in this region due to the high level of noise in the raw measurements. It can be seen that, for 2mm sample thickness that μ_a does not hold any relation with the biomass whereas the data obtained using 4mm thick sample shows an increase in the absorption coefficient with the increasing biomass, but the relationship is weaker compared to that at 1050nm.

The consistency in the extracted values for all three samples thicknesses indicates the reliability of the inversion method. Also this points to the potential of obtaining robust calibration models built on the extracted μ_a for absorbing species in the mixture (e.g. glucose) provided the errors in the extracted values are sufficiently low. Work on model suspensions[8,9] have shown that the models built by separating the absorption and scattering effects by extracting bulk optical properties and then building a calibration model using the bulk absorption coefficient can lead to significant improvement in performance. In addition to an improvement in performance, as discussed in the previous section, models built on μ_a have the potential to be easily transferred due to the fact that this is a fundamental property of the sample.

CONCLUSIONS

We have monitored bacterial growth by extracting near-infrared bulk optical properties. We observed that reflectance measurements vary nonlinearly with sample thickness in the second overtone region where scattering effects are dominant. This appears to be due to the competing effects of the absorption of photons as the sample thickness increases and the light reflected from the rear end on the cuvette. It was also seen that amount of information contained in reflectance measurements in the first overtone region decreases with increasing sample thickness, as indicated by the flattening of the reflectance profile in this region. While the relationship between reflectance and biomass in the scattering dominated region changes with sample thickness, and the intensity (absorbance) levels vary significantly for both reflectance and transmittance measurements, the extracted optical properties show consistent behavior both in terms of the relationship with biomass and magnitude. This observation indicates a potential for using the bulk optical properties of the

11

culture for building models that could be more easily transferable compared to those built using raw measurements.

[1] E. Dzhongova, C. R. Harwood, S. N. Thennadil, Applied Spectroscopy **63**, 1, 25 (2009).

[2] C. R. Harwood, S. M. Cutting, *Molecular Biology Methods for Bacillus* (John Wiley & Sons Ltd., 1990).

[3] S. A. Prahl, "The Adding-Doubling Method," in *Optical Thermal Response of Laser Irradiated Tissue*, A. J. Welch, v. G. M. J. C., eds. (Plenum Press, New York, 1995).

[4] W. Saeys, M. Velazco-Roa, S. Thennadil, H. Ramon, B. Nikolai, Applied Optics **47**, 7, 908 (2008).

[5] M. A. Velazco-Roa , S. N. Thennadil, Applied Optics **46**, 18, 3730 (2007).

[6] Z. Ge, A. Cavinato, J. Callis, Analytical Chemistry **66,** 1354 (1994).

[7] B. Beauvoit, H. Liu, K. Kang, P. D. Kaplan, M. Miwa, B. Chance, Cell Biophys **23**(1-3), 91 (1993).

[8] R. Steponavicius, S. N. Thennadil, Analytical Chemistry **81**, 7713 (2009).

[9] R. Steponavicius, S. N. Thennadil, Analytical Chemistry **83,** 1931 (2011).
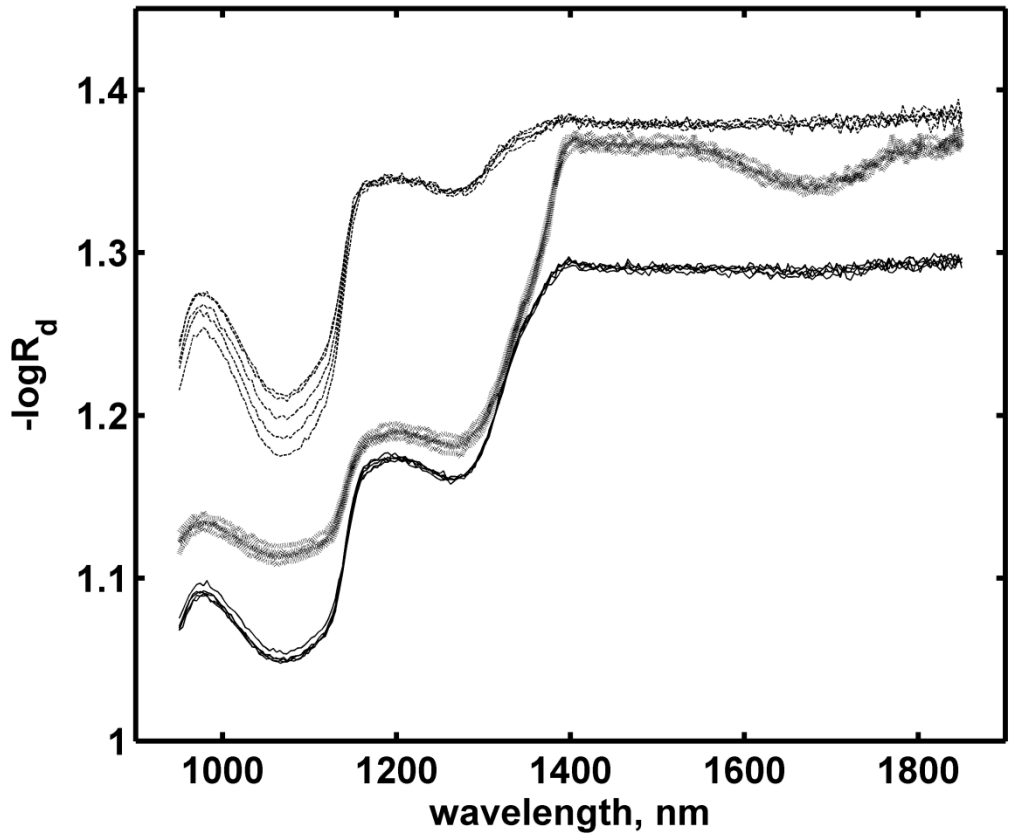
List of Figure Captions

Figure 1. Diffuse reflectance spectra taken during growth phase at different sample thicknesses (2mm, dotted line, 4mm solid line, and 10mm dashed line).
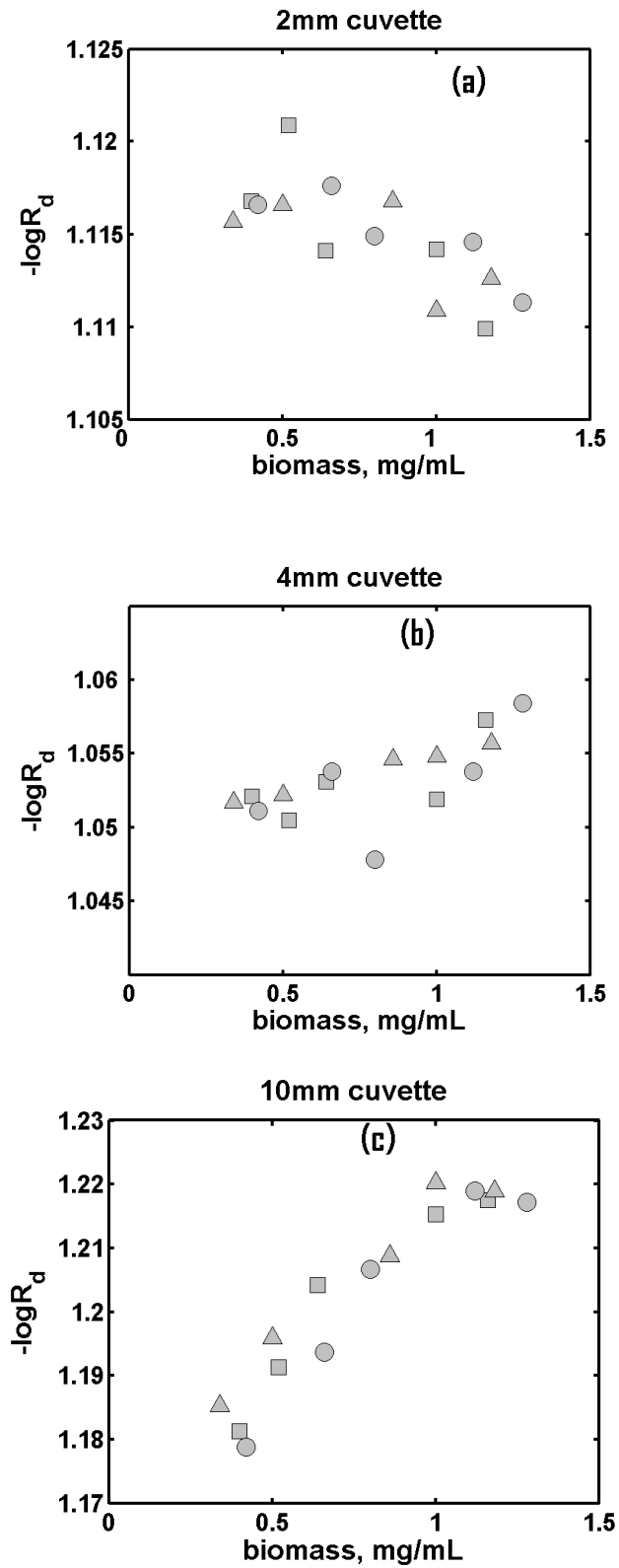
Figure 2. Total diffuse reflectance measurements (-logRd) at 1050nm during growth phase for three cultivations [run 1, triangles, run 2, circles run 3, squares] versus biomass for different sample thicknesses. (a) 2mm, (b) 4mm, (c) 10mm.

Figure 3. Total diffuse reflectance measurements (-logRd) at 1602nm during growth phase for three cultivations [run 1, triangles, run 2, circles run 3, squares] versus biomass for different sample thicknesses (a) 2mm, (b) 4mm, (c) 10mm.

Figure 4. Diffuse transmittance spectra taken during growth phase at different sample thicknesses (2mm, dotted line, 4mm solid line, and 10mm dashed line).

Figure 5. Total diffuse transmittance measurements (-logTd) at 1050nm during growth phase for three cultivations [run 1, triangles, run 2, circles run 3, squares] versus biomass for different sample thicknesses (a) 2mm, (b) 4mm, (c) 10mm.

Figure 6. Total diffuse transmittance measurements (-logTd) at 1602nm during growth phase for three cultivations [run 1, triangles, run 2, circles run 3, squares] versus biomass for different sample thicknesses. (a) 2mm, (b) 4mm, (c) 10mm.

Figure 7. Estimated bulk scattering coefficients during growth phase at different samples thickness (2mm, dotted line, 4mm solid line, and 10mm dashed line).

Figure 8. Estimated bulk scattering coefficient at 1050nm during growth phase for three cultivations [run 1, stars, run 2, circles run 3, triangles] versus biomass for different sample thicknesses. (a) 2mm, (b) 4mm, (c) 10mm.

Figure 9. Estimated bulk scattering coefficient at 1602nm during growth phase for three cultivations [run 1, triangles, run 2, circles run 3, squares] versus biomass for different sample thicknesses. (a) 2mm, (b) 4mm.

Figure 10. Estimated bulk absorption coefficients during the growth phase of the cultivation and at different samples thicknesses (2mm, dotted line, 4mm solid line, and 10mm dashed line).

Figure 11. Estimated bulk absorption coefficient at 1050nm during growth phase for three cultivations [run 1, triangles, run 2, circles run 3, squares] versus biomass for different sample thicknesses. (a) 2mm, (b) 4mm, (c) 10mm.
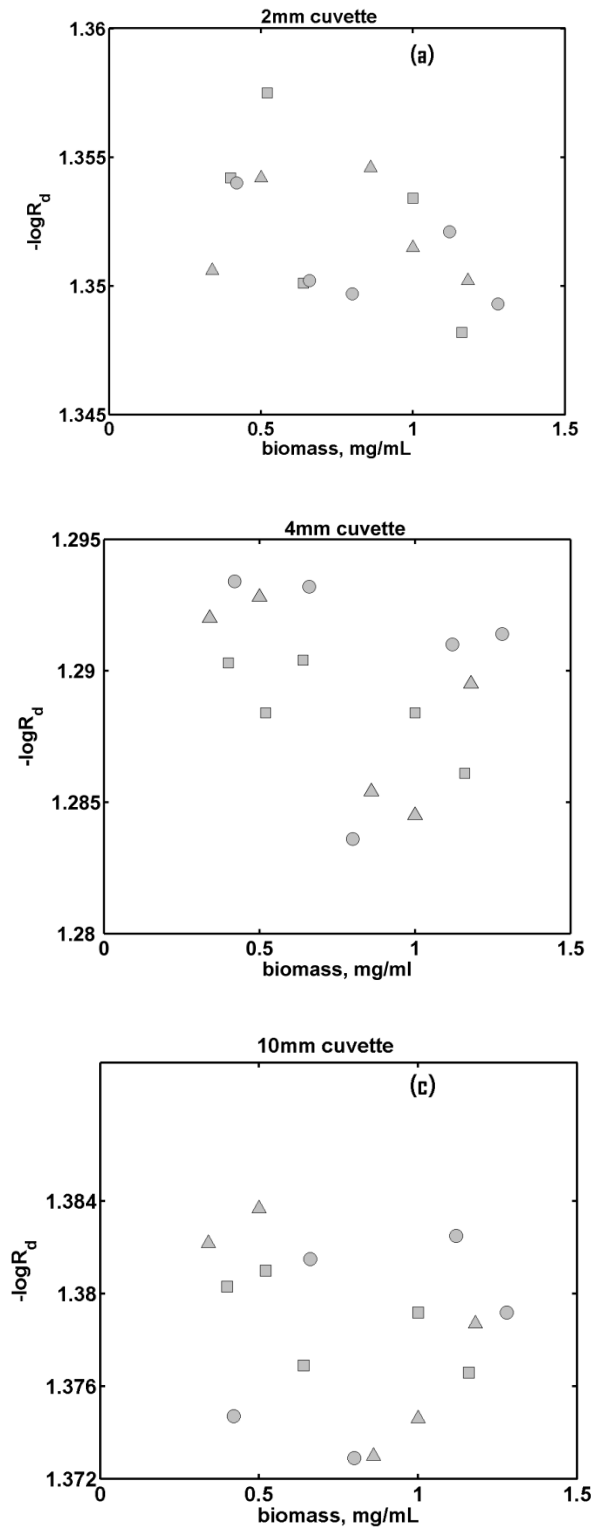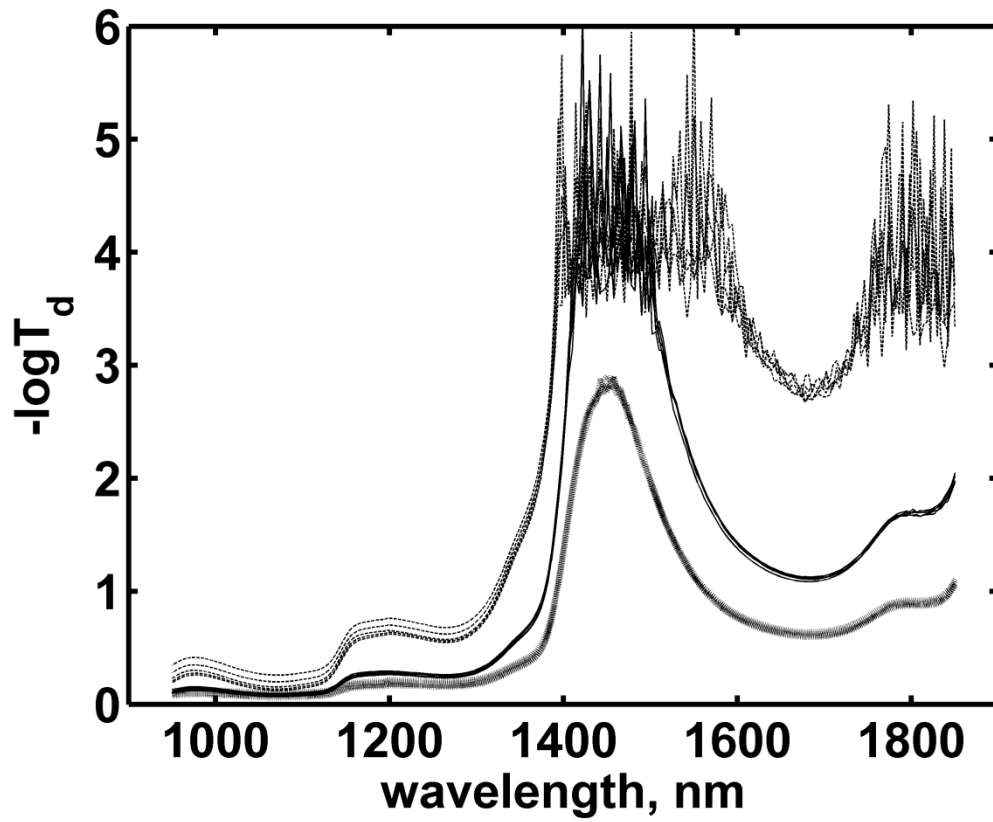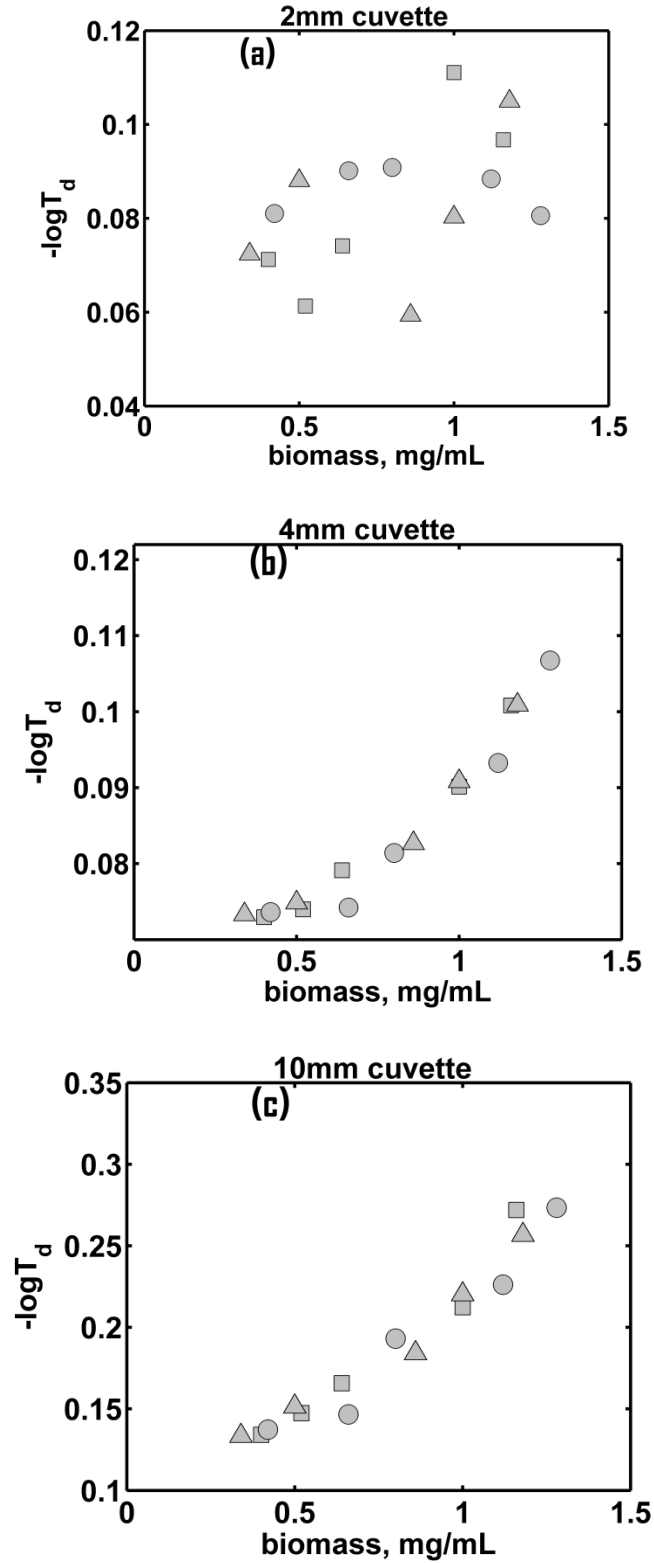
Figure 12. Estimated bulk absorption coefficient at 1602nm during growth phase for three cultivations [run 1, triangles, run 2, circles run 3, squares] versus biomass for different sample thicknesses. (a) 2mm, (b) 4mm.

Figure 1. Diffuse reflectance spectra taken during growth phase at different sample thicknesses (2mm, dotted line, 4mm solid line, and 10mm dashed line).

Figure 2. Total diffuse reflectance measurements (-logRd) at 1050nm during growth phase for three cultivations [run 1, triangles, run 2, circles run 3, squares] versus biomass for different sample thicknesses. (a) 2mm, (b) 4mm, (c) 10mm.
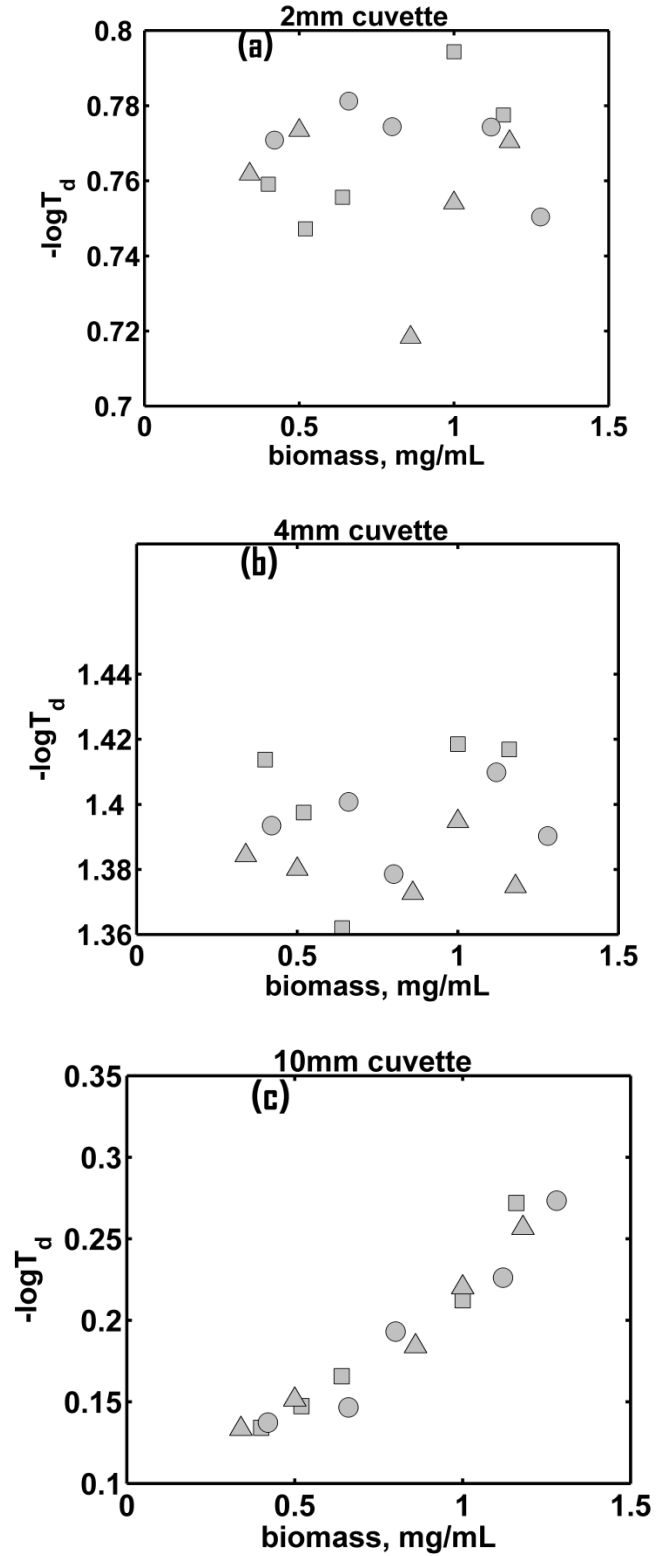
Figure 3. Total diffuse reflectance measurements (-logRd) at 1602nm during growth phase for three cultivations [run 1, triangles, run 2, circles run 3, squares] versus biomass for different sample thicknesses (a) 2mm, (b) 4mm, (c) 10mm.
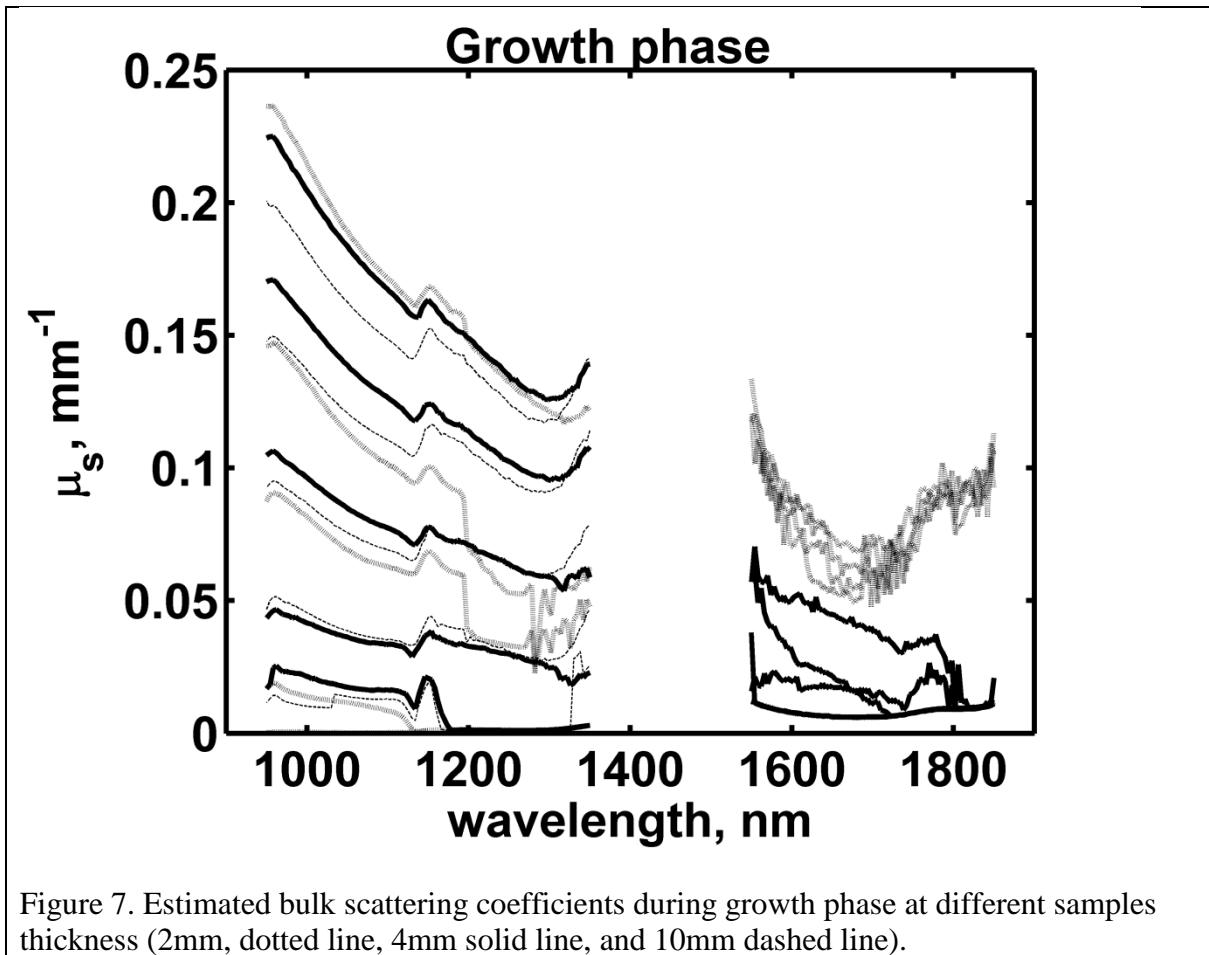
Figure 4. Diffuse transmittance spectra taken during growth phase at different sample thicknesses (2mm, dotted line, 4mm solid line, and 10mm dashed line).

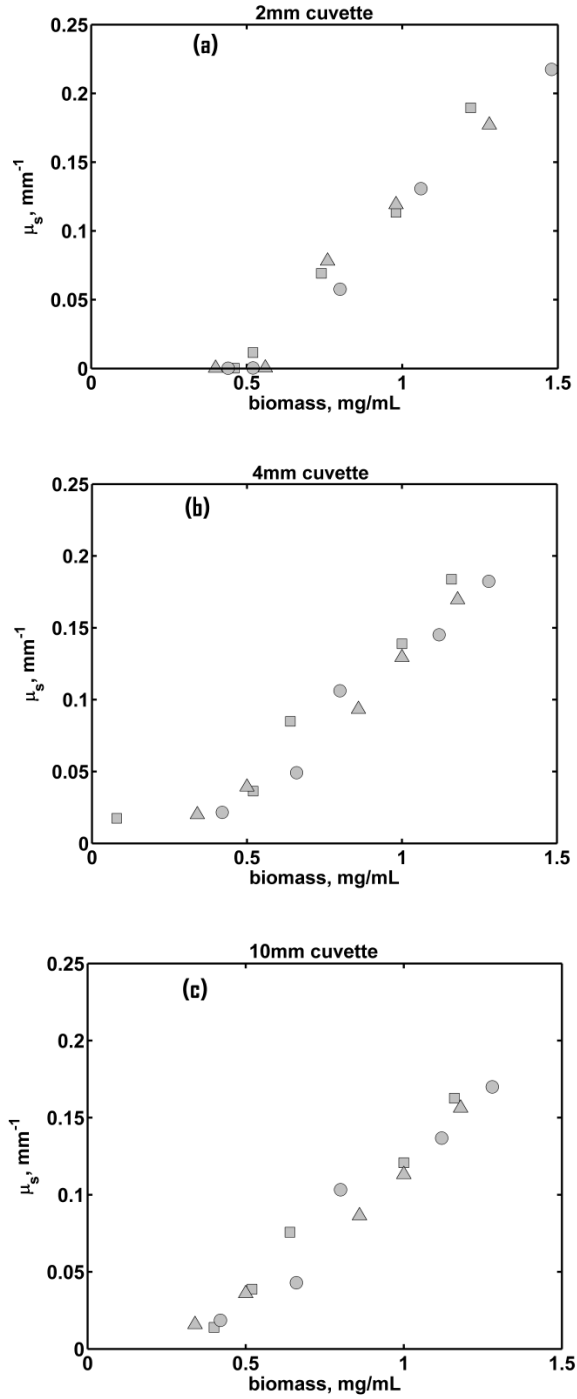Figure 5. Total diffuse transmittance measurements (-logTd) at 1050nm during growth phase for three cultivations [run 1, triangles, run 2, circles run 3, squares] versus biomass for different sample thicknesses (a) 2mm, (b) 4mm, (c) 10mm.

Figure 6. Total diffuse transmittance measurements (-logTd) at 1602nm during growth phase for three cultivations [run 1, triangles, run 2, circles run 3, squares] versus biomass for different sample thicknesses. (a) 2mm, (b) 4mm, (c) 10mm.

Figure 7. Estimated bulk scattering coefficients during growth phase at different samples thickness (2mm, dotted line, 4mm solid line, and 10mm dashed line).

Figure 8. Estimated bulk scattering coefficient at 1050nm during growth phase for three cultivations [run 1, stars, run 2, circles run 3, triangles] versus biomass for different sample thicknesses. (a) 2mm, (b) 4mm, (c) 10mm.
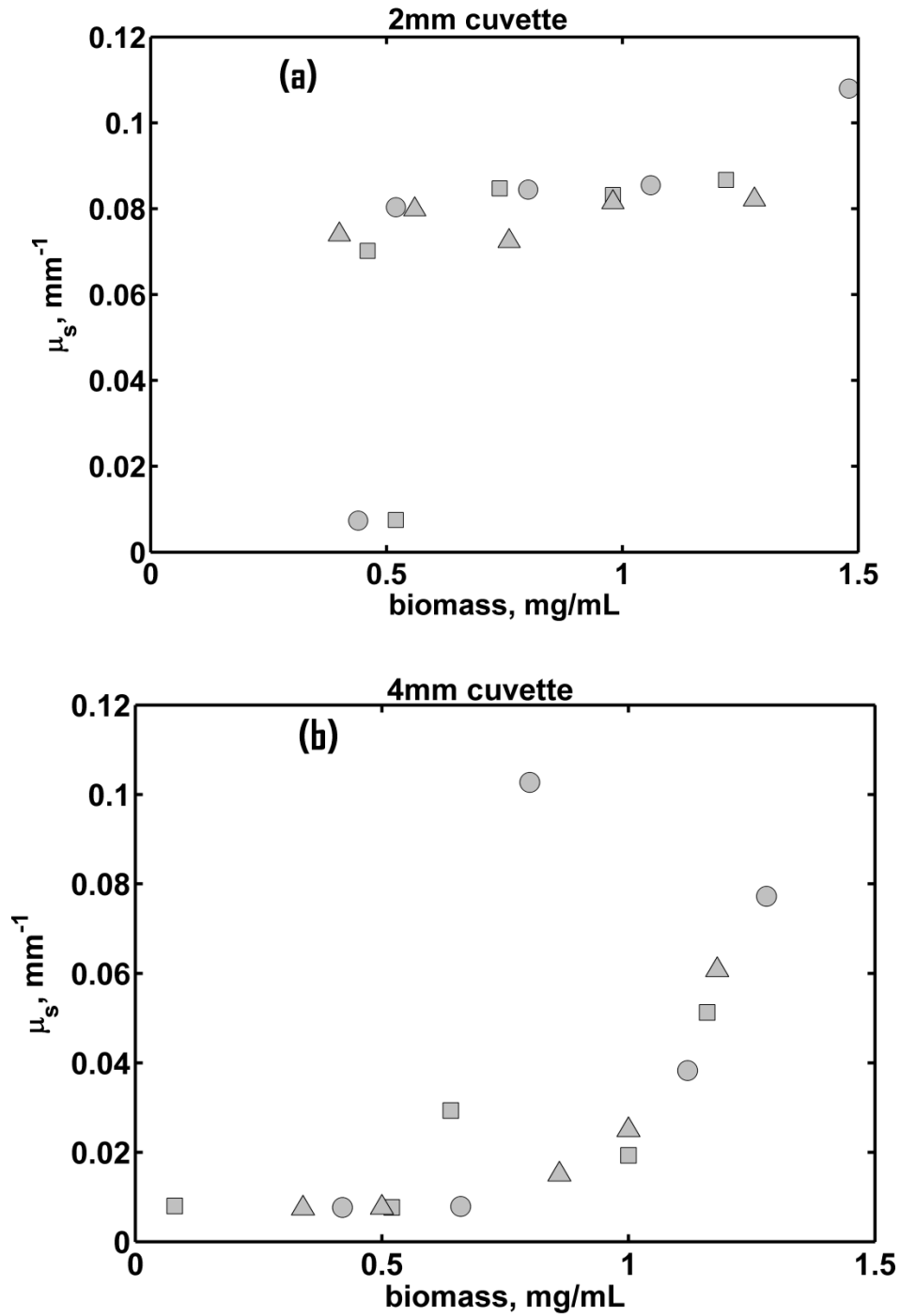
Figure 9. Estimated bulk scattering coefficient at 1602nm during growth phase for three cultivations [run 1, triangles, run 2, circles run 3, squares] versus biomass for different sample thicknesses. (a) 2mm, (b) 4mm.
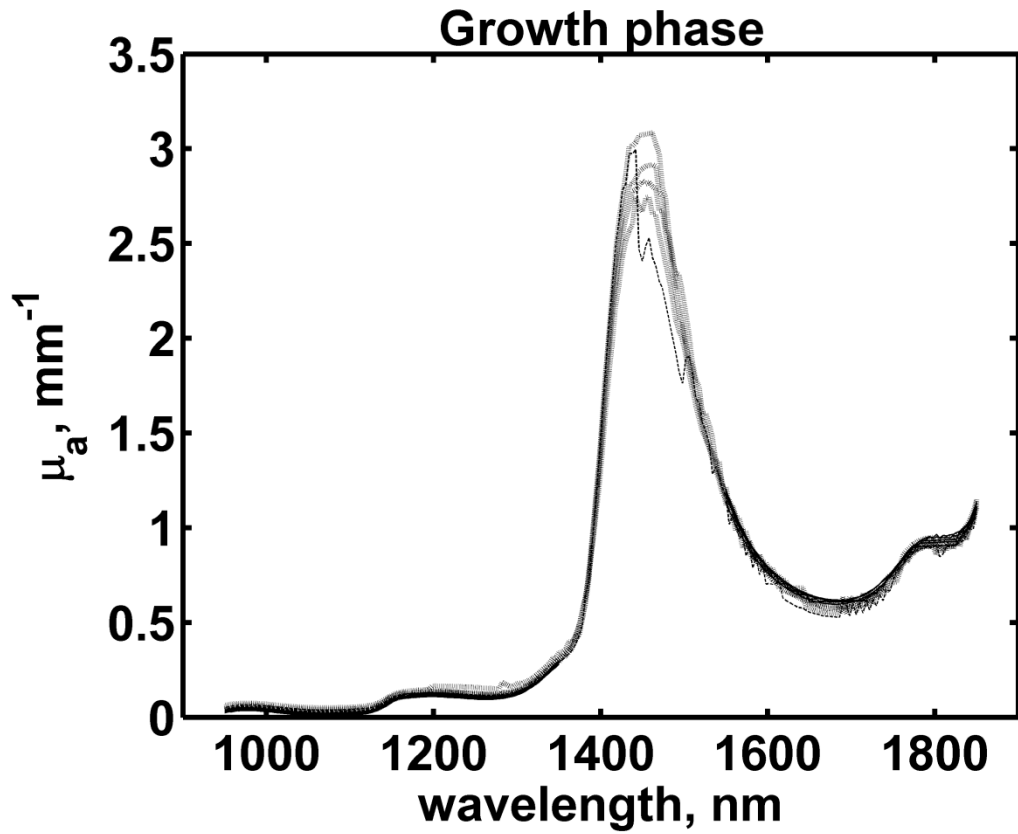
Figure 10. Estimated bulk absorption coefficients during the growth phase of the cultivation and at different samples thicknesses (2mm, dotted line, 4mm solid line, and 10mm dashed line).
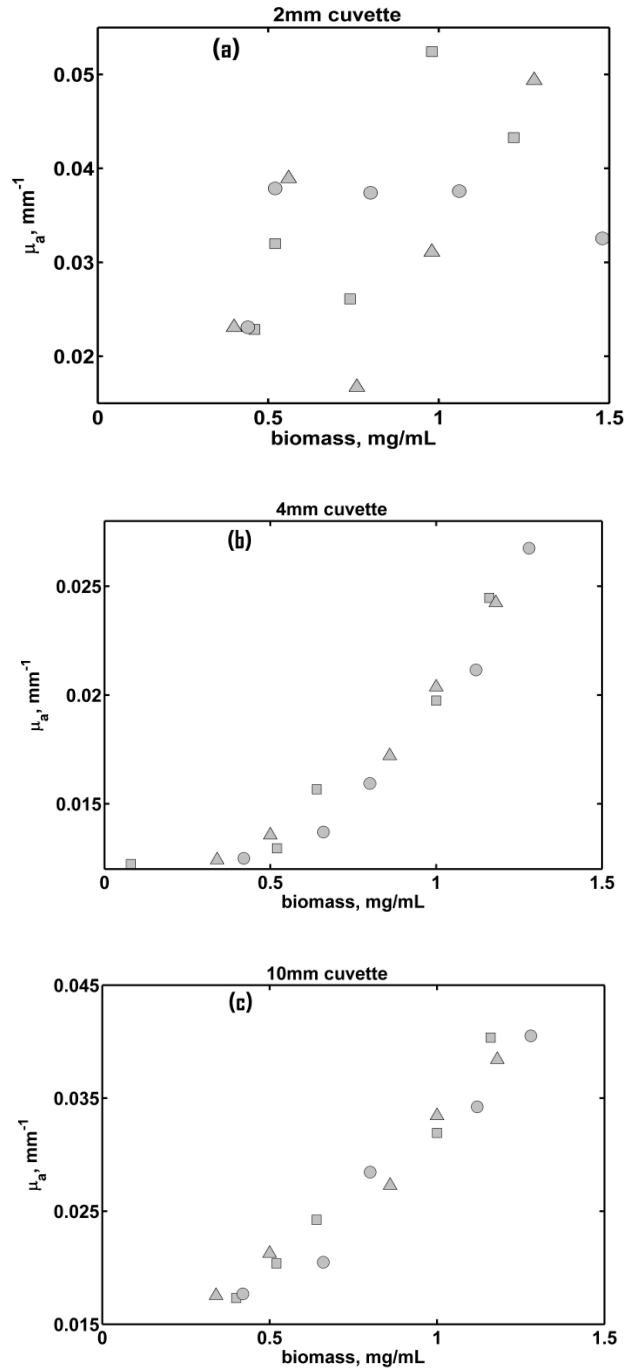
Figure 11. Estimated bulk absorption coefficient at 1050nm during growth phase for three cultivations [run 1, triangles, run 2, circles run 3, squares] versus biomass for different sample thicknesses. (a) 2mm, (b) 4mm, (c) 10mm.
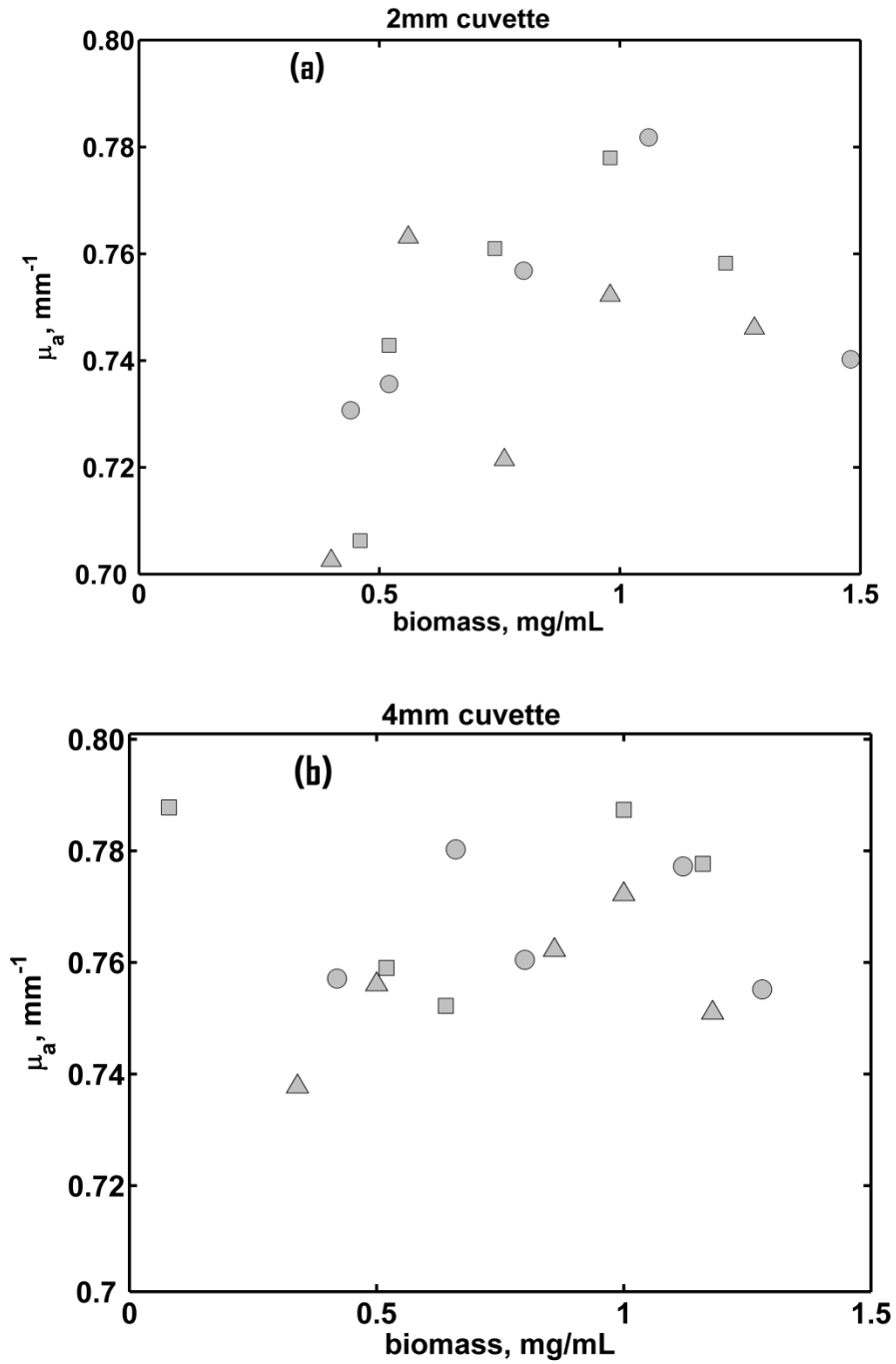
Figure 12. Estimated bulk absorption coefficient at 1602nm during growth phase for three cultivations [run 1, triangles, run 2, circles run 3, squares] versus biomass for different sample thicknesses. (a) 2mm, (b) 4mm.